

LES of Turbulent Flows: Lecture 15

(ME EN 7960-003)

Prof. Rob Stoll
Department of Mechanical Engineering
University of Utah

Fall 2014

Evaluating Simulations and SGS models

- How do we go about testing our models? How should models be validated and compared to each other?
- Pope (2004) gives 5 criteria for evaluating SGS models:
 1. Level of description in the SGS model
 2. Completeness of the model
 3. The cost and ease of use of the model
 4. The range and applicability of the model
 5. The accuracy of the model
- Most of these criteria are related to the accuracy of simulation results:
 - Accuracy**: Ability of the model to reproduce DNS, experimental or theoretical statistical features of a given test flow (or the ability to converge to these values with increasing resolution)

An important aspect of this is **grid convergence of simulation statistics**. This is not always done but is an important aspect of simulation validation. Note that this convergence (especially in high-Re flows) may not be exact, we may only see approximate convergence.

Evaluating Simulations and SGS models

-**Cost**: When examining the above, it is important to include the cost of each model (and comparisons between alternative models).

-One model may give better results at a lower grid resolution (larger Δ) but include costs that are excessive:

Example: Scale-dependent Lagrangian dynamic model (Stoll and Porté-Agel, WRR, 2006):

38% increase in cost over constant Smagorinsky model

15% increase over plane averaged scale-dependent model

How much of a resolution increase can we get in each direction for a 30% cost increase?? Only a little more than 3% in each direction!

-**Completeness**: A “complete” LES and SGS model would be one that can handle different flows with simply different specification of BCs, initial conditions and forcings.

-In general LES models are not complete due to grid requirements and (possibly) ad hoc tuning for different flows.

-Example from RANS: mixing length models are incomplete (different flow different l) while the k- ϵ model can be thought of as complete for RANS since it can be applied to any flow.

Evaluating Simulations and SGS models

Examples in the text books:

- Geurts chapter 8 (8.4 in particular)
- Sagaut 3rd ed. chapter 14 (several flows)

Test Case: Turbulent Boundary Layers

- An example from Guerts, 2004 of the effect of different SGS models on boundary layer development

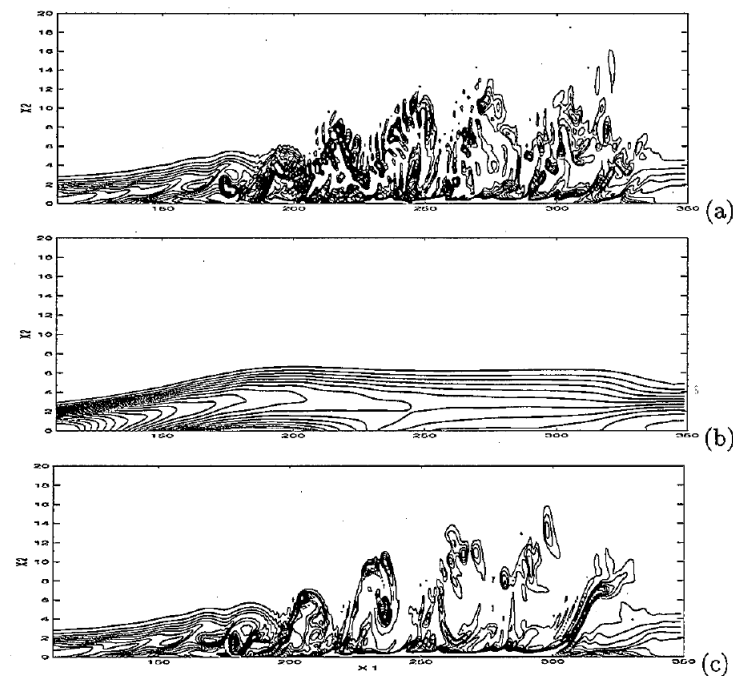


Fig. 8.15. Snapshot of the spanwise vorticity component: (a) DNS prediction, (b) LES with Smagorinsky's model and van Driest damping, (c) LES with dynamic eddy-viscosity model.

Test Case: Backward Facing Step

- An example from Cabot and Moin, 2000

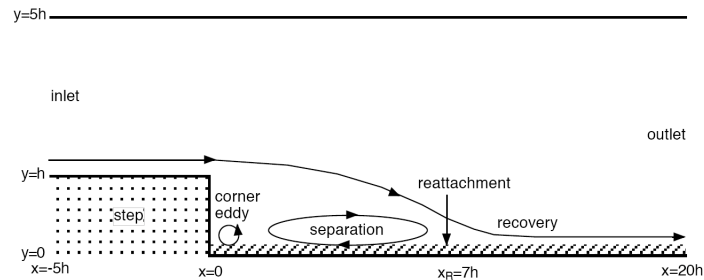


Figure 4. Sketch of the simulation domain for flow over a step of height h with an expansion ratio of 4 to 5. Wall stress models were used in the hatched region.

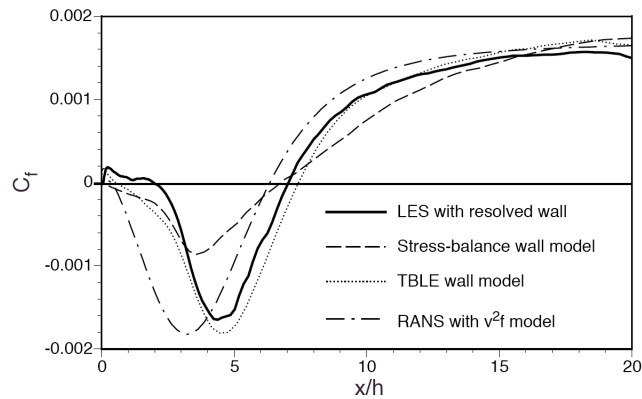


Figure 6. Friction coefficient on the bottom wall behind a step for the wall-resolved LES [2], wall stress models using stress balance and TBLE with a dynamic kappa in equation (5), and a global RANS v^2f model [18].

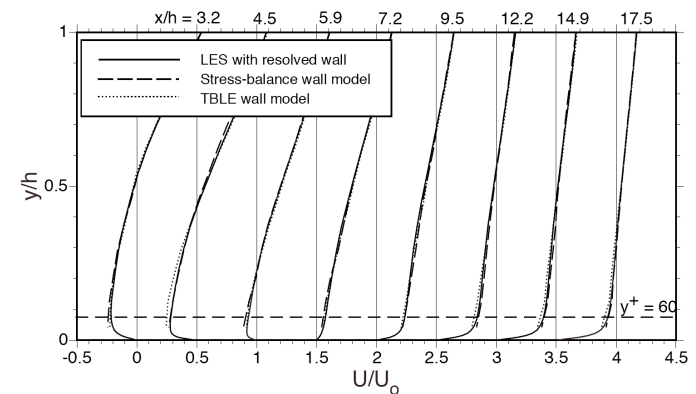


Figure 7. Mean streamwise velocity at different stations behind a step for the wall-resolved LES [2], and stress-balance and TBLE wall stress models. The dashed line is the height of the first computational cell, about 60 wall units near the exit.

Test Case: Mixing layer

- An example from Geurts
- Velocity spectra from DNS

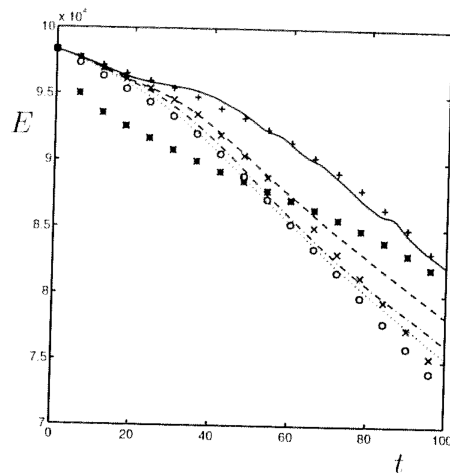


Fig. 8.5. Comparison of the total kinetic energy E obtained from the filtered DNS (marker o) and from LES using M0-6 (see table 8.2 for labels). From [221]

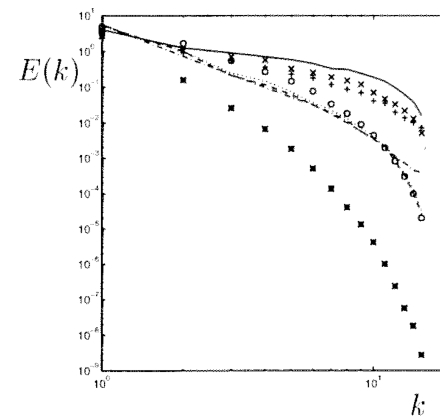


Fig. 8.6. Comparison of the streamwise energy spectrum $E(k)$ at $t = 80$ obtained from the filtered DNS (marker o) and from LES using M0-6 (see table 8.2 for labels). From [221].

Test Case: Mixing layer

- An example from Geurts
- Velocity spectra from DNS

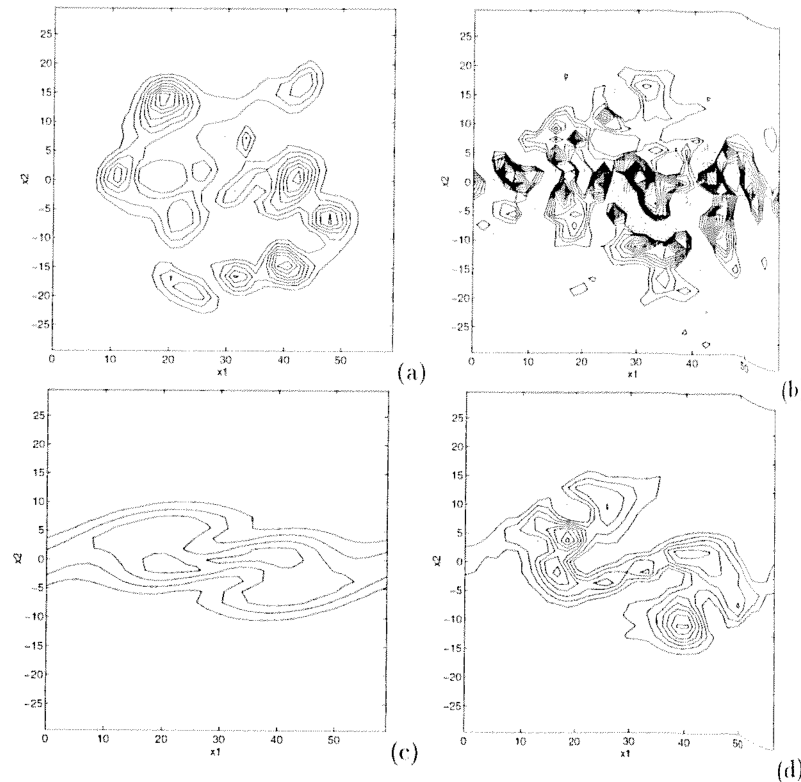
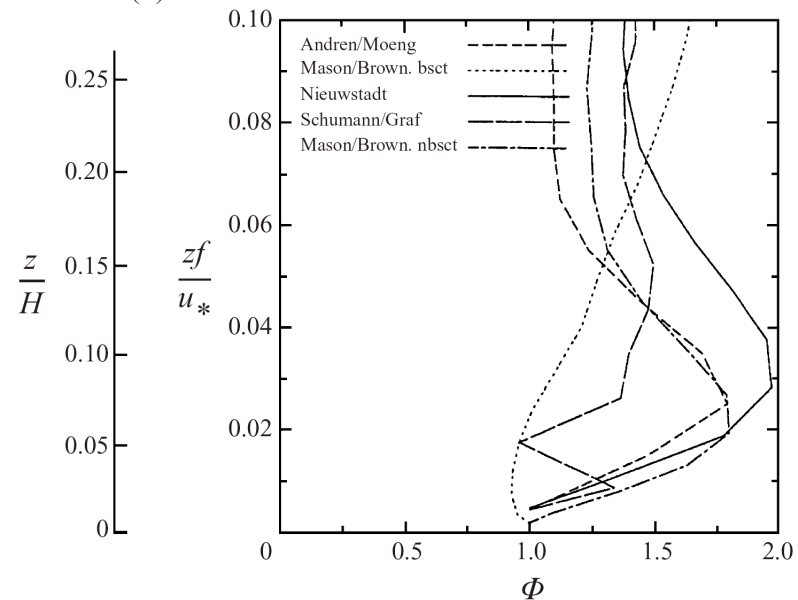
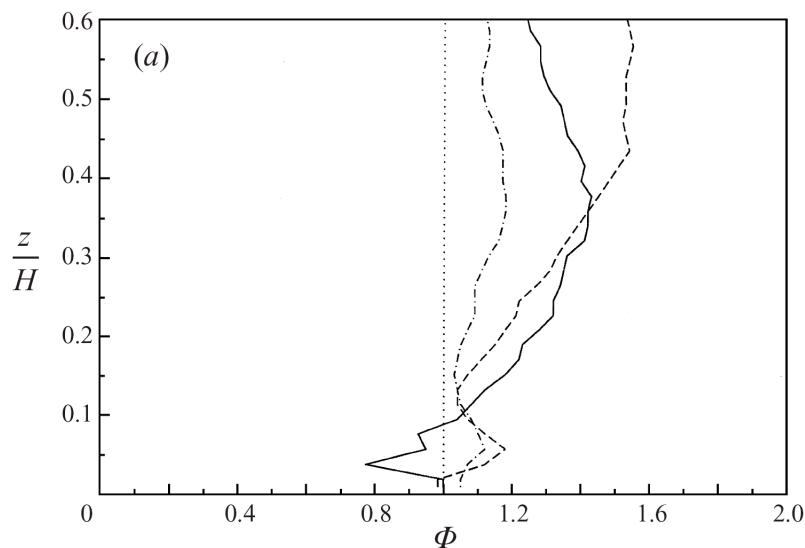


Fig. 8.7. Contours of spanwise vorticity for the plane $x_3 = 3\ell/4$ at $t=80$ obtained from (a) the filtered DNS, restricted to the 32^3 -grid, and from LES using (b) M0, (c) M1 and (d) M4. Solid and dotted contours indicate negative and positive vorticity respectively. The contour increment is 0.05. From [221].

Accuracy of LES models

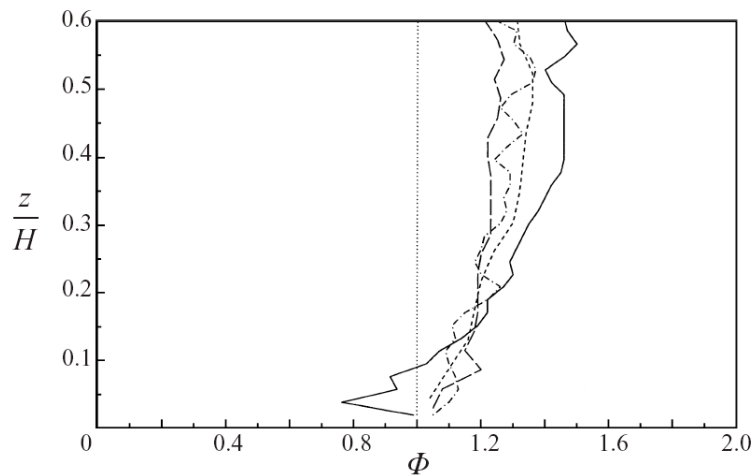
- Here we will look at some examples of different measurements of simulation accuracy and evaluation as well as a few common test cases for LES
- An example of the accuracy of LES models to predict flow statistics (from Porte-Agel et al, JFM 2000 and Andren et al., 1994, QJRMS):



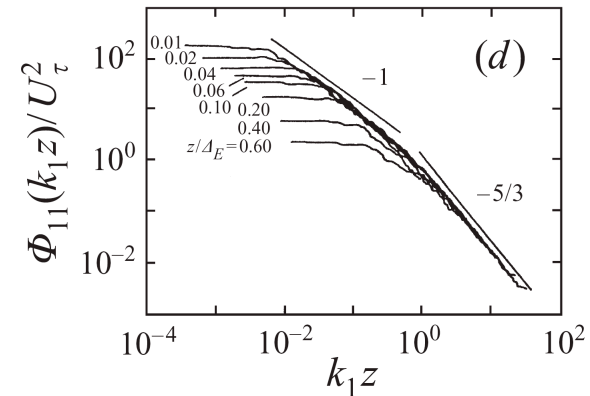
- Non-dimensional velocity gradient

Accuracy of LES models

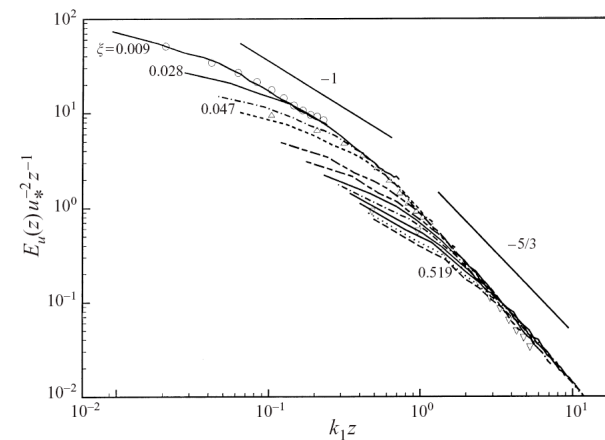
- An example of the accuracy of LES models to predict flow statistics (from Porte-Agel et al, JFM 2000)



- Non-dimensional velocity gradient



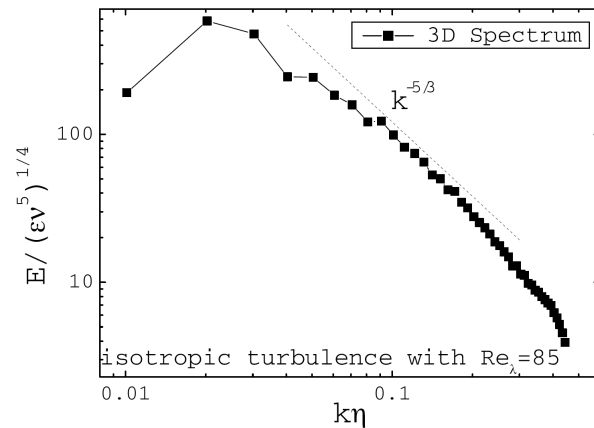
- Streamwise velocity spectra from Perry et al (1986)



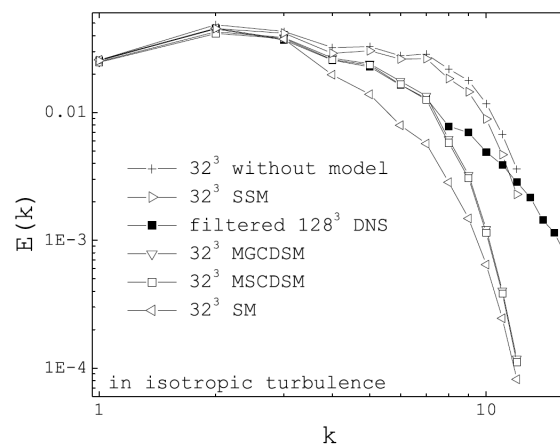
- Streamwise velocity spectra at two different resolutions

Test Case: Isotropic Turbulence LES

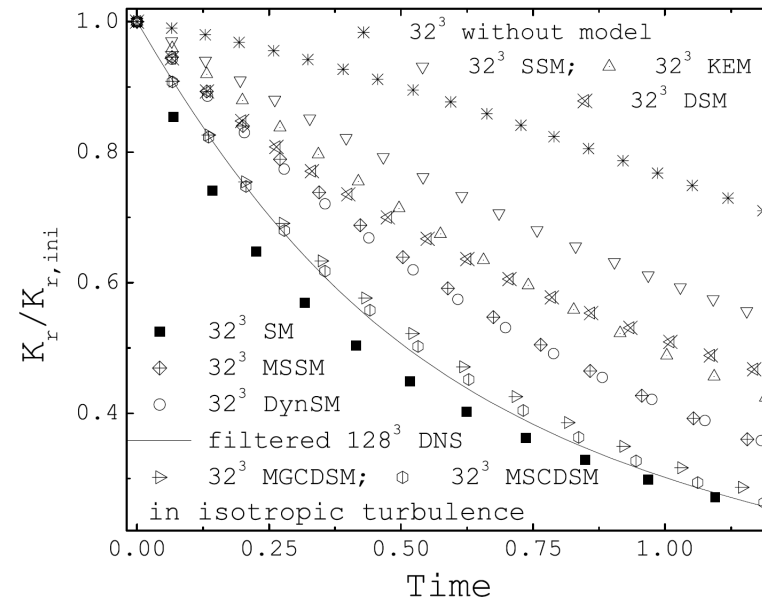
- An example from Lu et al, 2008



- Velocity spectra from DNS



- Velocity spectra from filtered DNS and LES



- Energy decay in isotropic turbulence

Test Case: flow over a 2D hill

- An example from Wan et al, 2007

- Velocity comparison with data and different models

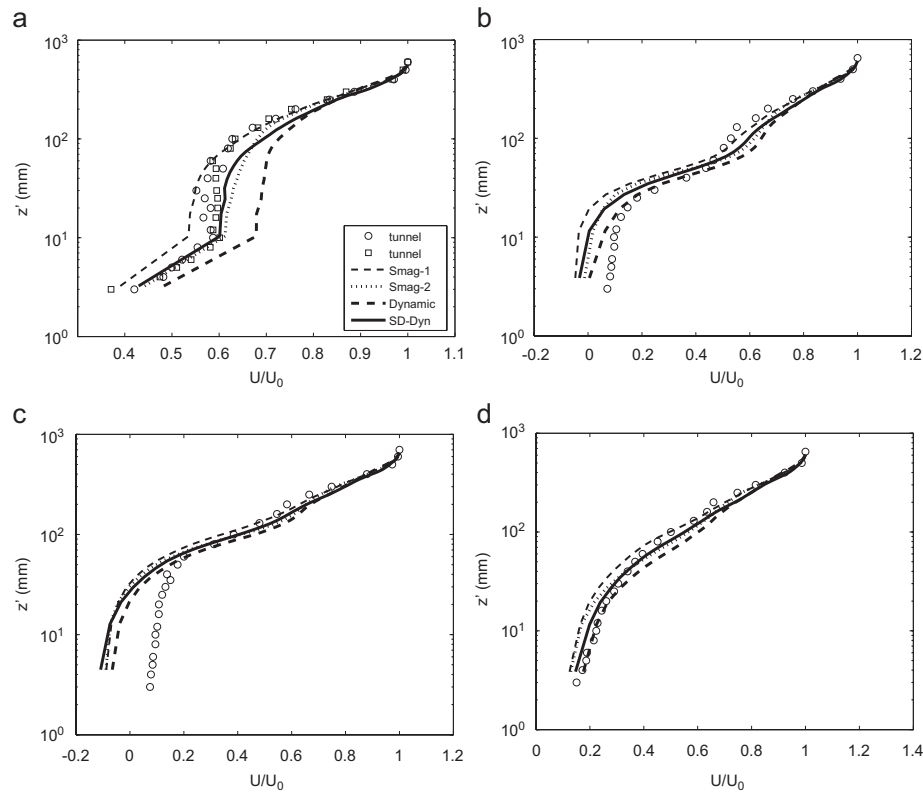


Fig. 2. Non-dimensional velocity profiles from wind tunnel data (symbols) and from LES with different SGS models: Smagorinsky model with two different matching functions (thin dashed and dotted lines), dynamic model (dashed line), and scale-dependent dynamic model (solid line). Results are presented for different positions in the flow: over the wave crests (a); over 1/4 wavelength downwind of the crest (b); over the wave trough (c); and over 1/4 wavelength downwind of the trough (d).

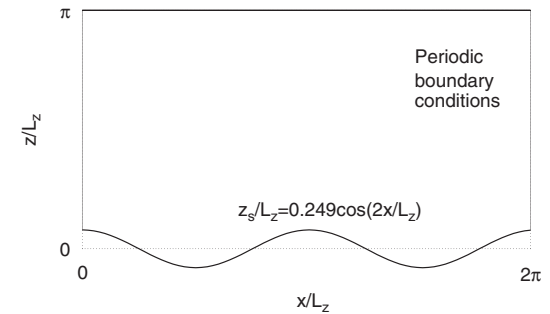


Fig. 1. Schematic of computational domain over the sinusoidal hill.

Test Case: flow over a 2D hill

- An example from Wan et al, 2007

- Velocity comparison with data and different models

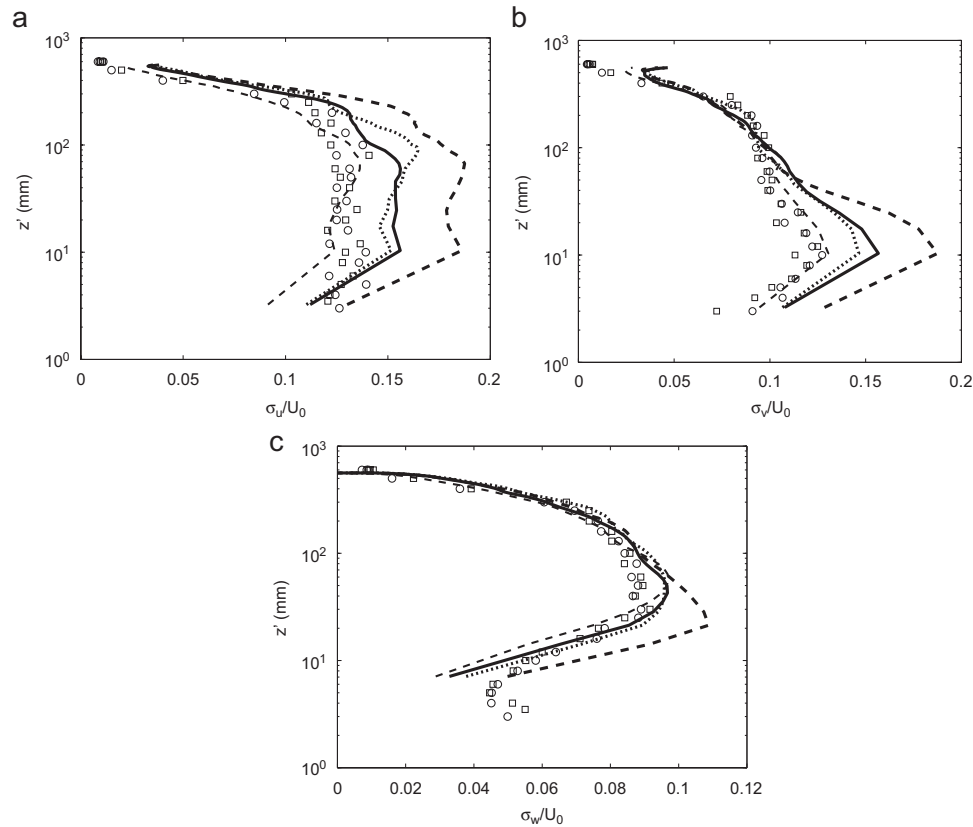


Fig. 3. Non-dimensional standard deviation of the resolved streamwise velocity from wind tunnel data (symbols) and from LES with different SGS models: Smagorinsky model with two different matching functions (thin dashed and dotted lines), dynamic model (dashed line), and scale-dependent dynamic model (solid line). Results are presented for different positions in the flow: over the wave crests (a); over 1/4 wavelength downwind of the crest (b); over the wave trough (c); and over 1/4 wavelength downwind of the trough (d).

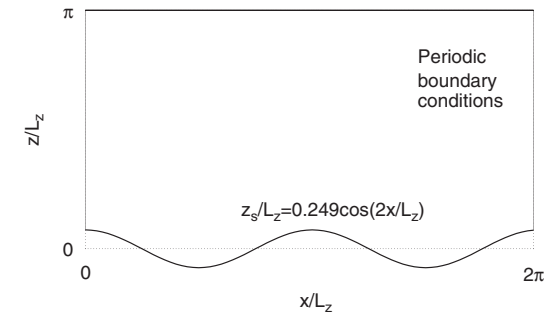


Fig. 1. Schematic of computational domain over the sinusoidal hill.

Example: Grid resolution

- An example from Sullivan and Patton, 2011
 - Re examined a typical flow used in atmospheric simulations as an analog for daytime conditions – high-Re weakly sheared convection.
 - Goal: understand mesh dependence of a particular SGS model (Deardorff, 1980 type, 1-equation)
- Domain: 5120 x 5120 x 2048 m (x,y,z)

TABLE 1. Simulation grid spacings.

Run	Grid points	$(\Delta x, \Delta y, \Delta z)$ (m)	Δ_f (m)
A	32^3	(160, 160, 64)	154
B	64^3	(80, 80, 32)	77.2
C	128^3	(40, 40, 16)	38.6
D	256^3	(20, 20, 8)	19.3
E	512^3	(10, 10, 4)	9.6
F	1024^3	(5, 5, 2)	4.8

Example: Grid resolution

- An example from Sullivan and Patton, 2011
- Domain: 5120 x 5120 x 2048 m (x,y,z)

TABLE 1. Simulation grid spacings.

Run	Grid points	($\Delta x, \Delta y, \Delta z$) (m)	Δ_f (m)
A	32^3	(160, 160, 64)	154
B	64^3	(80, 80, 32)	77.2
C	128^3	(40, 40, 16)	38.6
D	256^3	(20, 20, 8)	19.3
E	512^3	(10, 10, 4)	9.6
F	1024^3	(5, 5, 2)	4.8

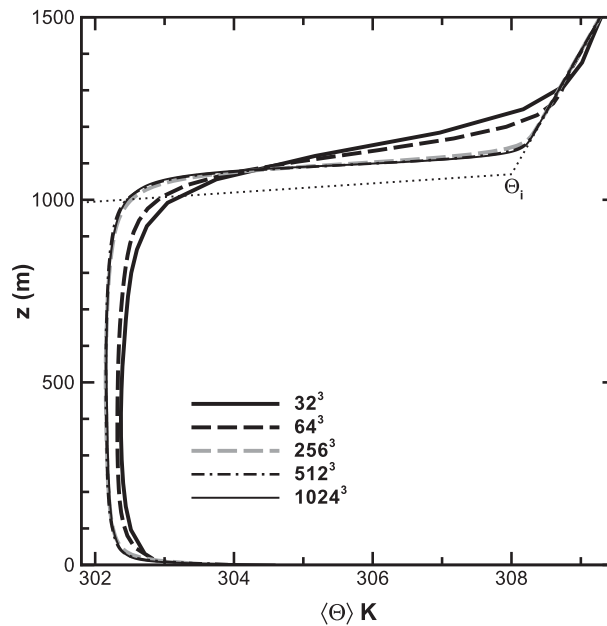


FIG. 2. Vertical profile of virtual potential temperature $\langle \bar{\theta} \rangle$ for varying mesh resolution. Note all simulations are started with the same three-layer structure for virtual potential temperature θ_i , indicated by the dotted line.

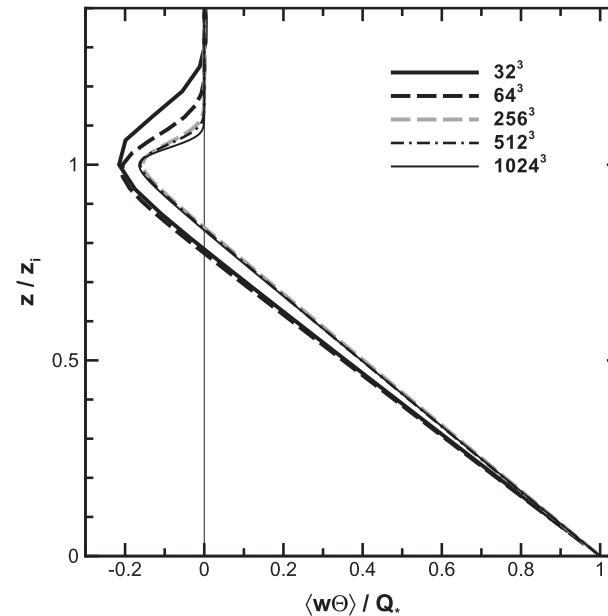


FIG. 3. Vertical profile of total temperature flux $\langle \bar{w}'\bar{\theta}' + \mathbf{B} \cdot \hat{\mathbf{k}} \rangle / Q_*$ for varying mesh resolution.

Example: Grid resolution

- An example from Sullivan and Patton, 2011
- Domain: 5120 x 5120 x 2048 m (x,y,z)

TABLE 1. Simulation grid spacings.

Run	Grid points	($\Delta x, \Delta y, \Delta z$) (m)	Δ_f (m)
A	32^3	(160, 160, 64)	154
B	64^3	(80, 80, 32)	77.2
C	128^3	(40, 40, 16)	38.6
D	256^3	(20, 20, 8)	19.3
E	512^3	(10, 10, 4)	9.6
F	1024^3	(5, 5, 2)	4.8

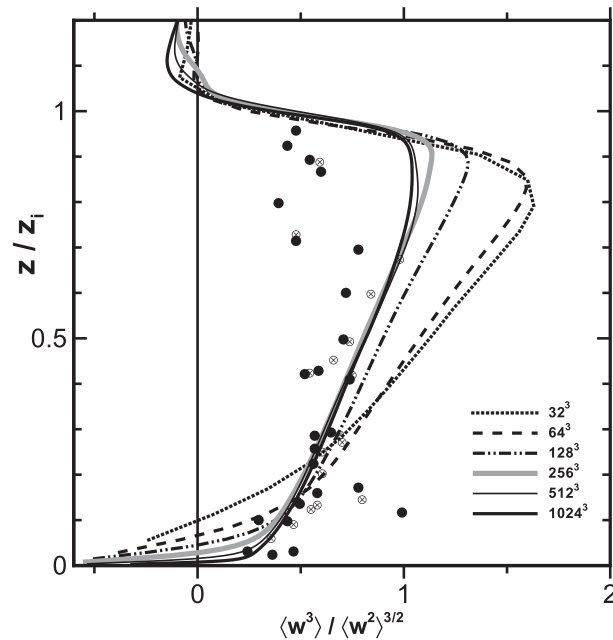


FIG. 9. Effect of mesh resolution on resolved vertical velocity skewness $S_{\bar{w}}$. The lines legend indicates the mesh size of the various simulations. The skewness is computed using the resolved (or filtered) vertical velocity field $\bar{w} = \bar{w}^r$. The observations are taken from the results provided in Moeng and Rotunno (1990).

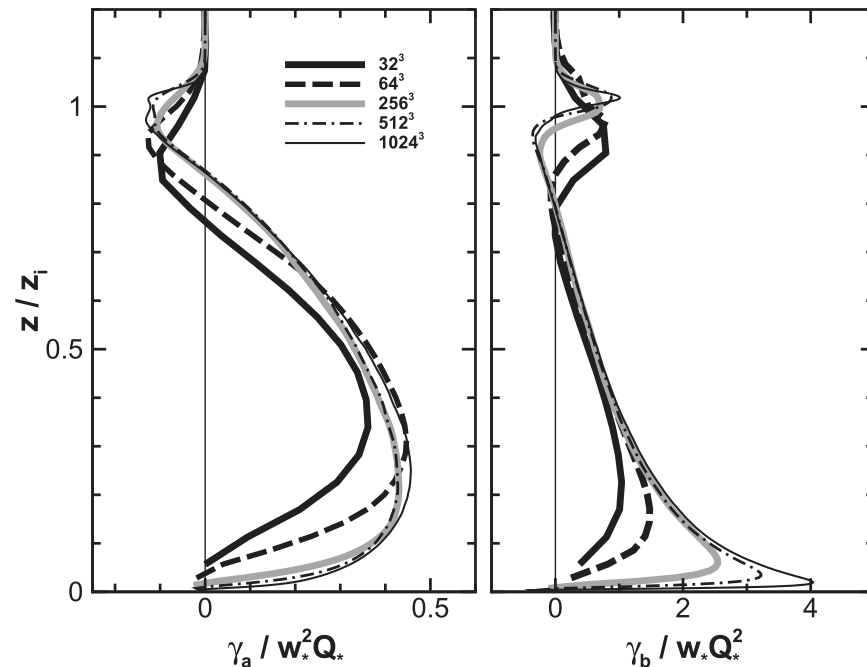


FIG. 12. Effect of mesh resolution on resolved third-order moments (left) $\gamma_a = \langle \bar{w}^2 \bar{\theta}^r \rangle$ and (right) $\gamma_b = \langle \bar{w}^r \bar{\theta}^r{}^2 \rangle$.